

Algorithm Theoretical Basis Document

Inversion of Bending Angle and Refractivity profiles

STAR ROPP Version 1.0 (Based on the ROPP Version 10.0)

1. Introduction

This document describes the algorithms used to derive the bending angle and refractivity products produced by the Radio Occultation Processing Package (ROPP) version 10 (ROPP user guide, 2020). We have modified the processing package to process the latest Radio Occultation (RO) missions, e.g., COSMIC-2 and Spire, referred to as STAR ROPP. The inputs to the algorithm are coordinates of the Global Navigation Satellite System (GNSS) and low Earth orbit (LEO) satellites in Earth Centered Inertial (ECI) coordinate systems, and the excess phases and the signal-to-noise ratios (SNR) of the Doppler shifted signal at two frequency bands. The frequency bands for Global Positioning System (GPS) include L1, centered at 1.57542 GHz, L2, centered at 1.2276 GHz, and L5, centered at 1.17645 GHz. These carrier frequencies are modulated with precision (P) and Coarse Acquisition (C/A) ranging codes. RO data processing generally uses L1C and L2C GPS bands for inversions. GLOBalnaya NAVigatsionnaya Sputnikovaya Sistema (GLONASS) transmits L1 and L2 band radio signals in the frequencies 1.5980625–1.6093125 GHz and 1.2429375–1.2516875 GHz, respectively. The GNSS carrier frequency of the E1 Galileo band is centered at 1.57542 GHz, the same center frequency as the GPS L1 band, but with a different bandwidth. The E5 band of Galileo has a central frequency of 1.20714 GHz. Besides GPS, GLONASS, and Galileo, modern GNSS receivers can track GNSS signals from BeiDou, Quazi Zenith Satellite System (QZSS), etc. The high-frequency bands (L1, E1) are the primary bands used in the GNSS RO data processing. Secondary bands (L2, E5) are used for ionospheric correction to retrieve neutral atmospheric refractivity profiles.

The produced products are bending angles at the two frequencies, their uncertainties in terms of local spectral width, ionospheric corrected bending angle as a function of impact parameter, and ionospheric corrected bending angle and refractivity as a function of height.

2. Inputs and initial data needed for the STAR ROPP

STAR ROPP converts RO excess phase data to bending angle and refractivity profile. Input excess phase and other auxiliary data are taken from level1b conPhs/atmPhs data. The RO conPhs (or atmPhs) file contains reconstructed full-resolution excess phase, occultation time, pseudo ranges, SNRs, orbit information (position and velocity), impact parameters, and quality information. Currently, we use RO conPhs/atmPhs generated by the University Corporation for Atmospheric Research (UCAR) operational data processing center and distributed by COSMIC Data Analysis and Archive Center (CDAAC). In the future, we could use RO conPhs/atmPhs files generated by the STAR GNSS RO team.

3. STAR ROPP approach, configuration, quality control

3.1 STAR ROPP approach

The conPhs/atmPhs file is first converted to the standard ROPP netCDF format as an input to ROPP processing. Since May 19, 2020 (day-of-year (DOY) 140), UCAR changed the conPhs format for COSMIC-2 and reduced the data volume by using low rate time for orbit-related variables such as GNSS and LEO positions and GNSS signal transmission. We have modified the ROPP input/output module to add the capability to interpolate orbit positions and signal transmission from the low time rate to the high time rate. We also added the capability into the ROPP package to process RO observations from multiple GNSS satellites, including GLONASS, GALILEO, and BeiDou, in addition to GPS, by updating the L1 and L2 frequencies based on different GNSS systems.

3.2 Configuration

We used wave optics, a canonical transform (CT2) algorithm (Gorbunov and Lauritsen, 2004), to derive bending angle as a function of impact parameter from excess phase as a function of time. The detailed configuration parameters to run the processing are given in Table 1.

Table 1: The configuration parameters:

Configuration n	Value	Description
0. Excess phase to bending angle processing		
occ_method	WO	use WAVE OPTICS (CT2 algorithm) processing to derive bending angle as a function of impact parameter from excess phase as a function of time
filter_method	slpoly	use SLIDING polynomial
fw_go_smooth	3000.0	Filter width for smoothed GO (Geometric Optics) bending angles (m)
fw_go_full	3000.0	Filter width for full resolution GO bending angles (m)
fw_wo	2000.0	Filter width for wave optics bending angle above 7 km (m)
fw_low	-1000.0	Filter width for wave optics bending angle below 7 km (m)
hmax_wo	25000.0	Maximum height for wave optics processing (m)
Acut	0.0	Fractional cut-off limit for amplitude
Pcut	-2000.0	The cut-off limit for impact height (m)
Bcut	0.1	The cut-off limit for bending angle (m)
Hcut	-250000	The cut-off limit for straight-line tangent altitude (m)
CFF	3	Complex field filter flag
dsh	200	Shadow border width (m)
1. Ionospheric correction processing		
method	GMSIS	use MSIS climatology bending angle (searching global MSIS profiles for the best fit profile to observation) in ionospheric correction, statistical optimization, and bending angle to refractivity inversion.

abel	LIN	Assume linear variation of bending angle and $\ln(n)$ between observation levels. This algorithm is used in ROM SAF NRT processing
so_method	so	Statistical optimization
2. Impact parameter grid		
dpi	100.0	Step of standard impact parameter grid (m)
3. Smoothing bending angle profile		
np_smooth	3	Polynomial degree for smoothing regression
fw_smooth	1000.0	Filter width for smoothing profile (m)
4. Model bending angle profile fit to observations		
sf_method	parallel	Search and fit method (parallel or serial)
nparm_fit	2	Number of parameters for model fit regression
hmin_fit	20000.0	The lower limit for model fit regression (m)
hmax_fit	70000.0	The upper limit for model fit regression (m)
5. Ionospheric correction and statistical optimization		
f_width	2000.0	Ionospheric correction filter width (m)
delta_p	20.0	Step of homogeneous impact parameter grid
s_smooth	2000.0	External ionospheric smoothing scale
z_ion	50000.0	Lower height limit of ionospheric signal (m)
z_str	35000.0	Lower height limit of stratospheric signal (m)
z_ltr	12000.0	Lower height limit of tropospheric signal (m)
n_smooth	11	Number of points for smoothing (must be odd)
model_err	-0.5	A priori model error standard deviation
6. Bending angle inversion to refractivity		
ztop_invert	150000	Height of atmosphere top for inversion (m)
dzh_invert	50.0	Step of inversion grid above observation top (m)
dzr_invert	20000.0	The interval for regression in inversion (m)

3.3 Quality control

The STAR ROPP algorithm quality control (QC) is based on identifying and flagging bending angle profiles with significant deviation from the climatology background. The primary objective of this quality control measure is to exclude outliers from the dataset.

We use ECMWF ERA5 six-hour forecast model atmospheric states (data available from <https://apps.ecmwf.int/data-catalogues/era5/?type=fc&class=ea&stream=oper&expver=1>) to simulate bending angles by using a RO forward model for each STAR ROPP profile. ERA5 gridded Temperature (T), specific humidity (q), geopotential height (Z), and pressure (P) are interpolated to the RO latitude, longitude, and time to calculate the bending angle (α) profiles as a function of altitude (z) and impact height (a) using Eqs. (1) – (4).

Water vapor pressure (e) is derived using specific humidity (q) and pressure (P)

$$e = P * \frac{q}{0.622+0.378*q} \quad (1)$$

The refractivity (N) is calculated as

$$N = 77.6 \frac{P}{T} + 3.73 \times 10^5 \frac{e}{T^2} \quad (2)$$

Altitude (z) is calculated from geopotential height (Z) using implementation derived from the Somigliana equation [see https://rom-saf.eumetsat.int/general-documents/gsr/gsr_02.pdf for details]. The model impact parameter (a) at altitude (z) is calculated as

$$a = n(R + z) \quad (3)$$

where the refractive index $n = 1 + N \times 10^{-6}$. The corresponding bending angle (α) profile can be calculated from n and a using Abel integration

$$\alpha(a) = 2a \int_{r_t}^{\infty} \frac{1}{\sqrt{n^2 r^2 - a^2}} \frac{d \ln(n)}{dr} dr \quad (4)$$

where $r_t = R + z$. R is the earth's radius at the occultation perigee point.

The fractional difference of the bending angle between RO observation (O) and ERA5 simulation (B) is calculated at each altitude level and used to estimate the quality of the RO data.

$$BA_{diff} = \frac{O-B}{B} \quad (5)$$

Figure 1 shows the monthly mean standard deviation of the fractional bending angle difference distribution as a function of altitude in 2020 between 8 to 43 km. We define σ_{year} as the yearly mean standard deviation for the whole year of 2020. All the profiles with bending angle fractional difference larger than $7 * \sigma_{year}$ at any given altitude level between 10 to 40 km altitudes, where RO data have the highest quality and different RO retrieval models are in excellent agreement, are flagged as 'bad'. A sensitivity study showed that $7 * \sigma_{year}$ value provides the optimized balance between quality-controlled (QCed) profile number and quality.

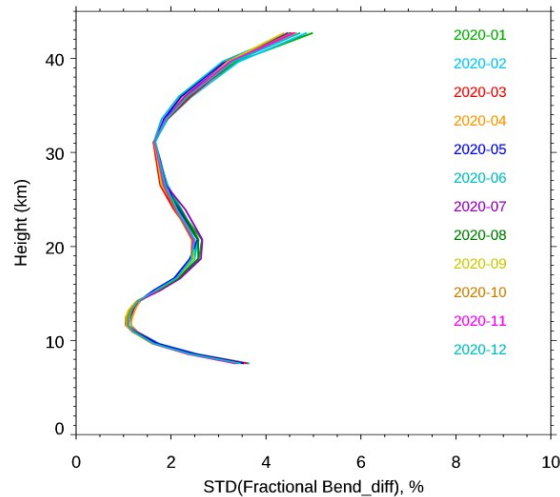


Figure 1. Monthly standard deviation of the fractional bending angle differences in 2020.

We also flag those profiles with several other existing abnormal characters. These reasons for flagging profiles as ‘bad’ are summarized below:

1. The model simulation is unavailable.
2. The fractional BA difference against reference is larger than $7 * \sigma_{year}$.
3. The altitude top height is lower than 20km.
4. The altitude bottom height is higher than 20km.
5. A negative bending angle below 50 km height is found.

It is important to note that the QC procedure exclusively utilizes bending angles within a specific height range (e.g., from 10 to 40 km). In some rare instances, while the bending angle falls within an acceptable range, anomalies in refractivity and/or dry temperature arise due to inadequacies in the Abel inversion calculations. For example, during its end-of-life phase starting from December 2022, KOMPSAT-5 showed discrepancies with the climate model regarding temperature and refractivity. The QC procedures will be further improved in the next version.

4. Initial validation results

4.1 Data quality and penetration height

To evaluate the STAR ROPP COSMIC-2 bending angle quality, we compare them with the UCAR COSMIC-2 bending angle. RO retrievals may vary when implementing different processing procedures. Figure 2 shows the relative bending angle difference between the STAR ROPP and UCAR COSMIC-2. The relative bending angle is close to zero from 8 km to 40 km. However, the bending angle difference (and standard deviation) significantly increases below 8 km.

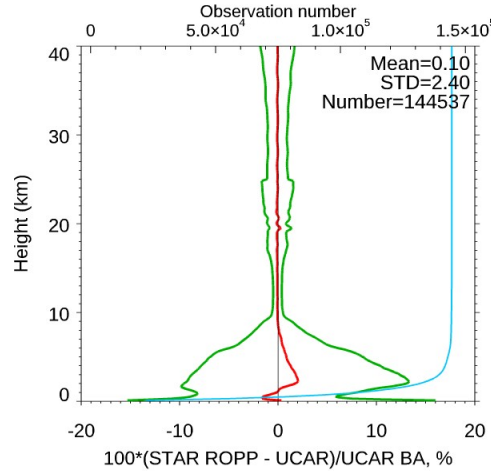


Figure 2. Bending angle profile comparison between STAR ROPP and UCAR COSMIC-2 for the mean difference (in red line), standard deviation (in green line), and the corresponding numbers of observations (in blue line) from surface to 40 km altitude. One month (July 1-31, 2022) of COSMIC-2 bending angle observations were used to generate this figure.

Similar to the quality control step, we interpolate the ERA5 simulated bending angle profiles onto the locations and times of the COSMIC-2 data. Figure 3 shows no noticeable difference for the COSMIC-2–ERA5 pairs in different processing procedures, i.e., STAR ROPP versus UCAR. The same month, from 1 to 31 July 2022, is used in the comparisons.

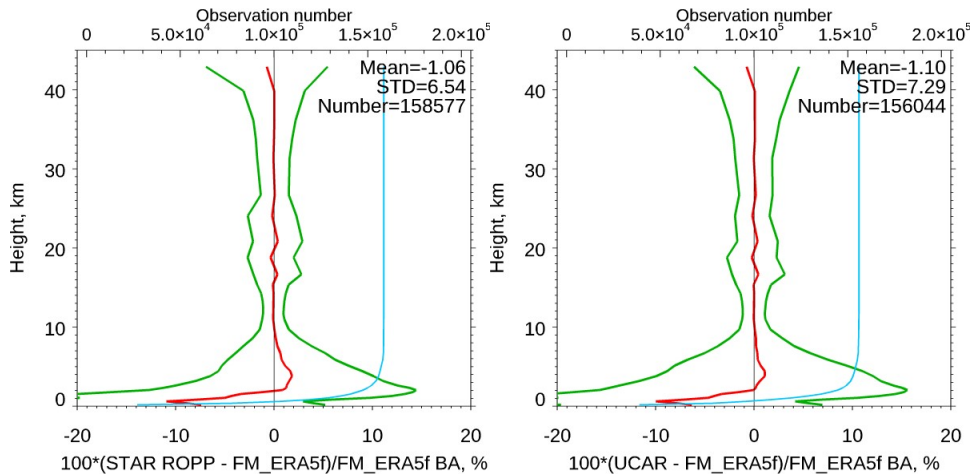


Figure 3. Fractional bending angle difference and penetration depth comparison. (a) STAR ROPP against ERA5 forecast and (b) UCAR against ERA5 forecast in July 2022.

In RO inversion procedures, it is essential to use RO tracking information and the derived excess phase to determine the cut-off height for RO retrievals. This ensures the optimal retrieval of the RO bending angles and refractivity profiles. Figure 4 depicts the penetration heights for COSMIC-2. It shows that above 2 km altitude, UCAR and STAR ROPP penetration heights are very close. Between 0.5 km and 1.5 km altitude, STAR ROPP penetration height is slightly deeper than that of UCAR and reverses below 0.5 km altitude. We believe that it is

related to the configuration parameter we chose. Optimization is underway to improve the STAR ROPP penetration height in the next version.

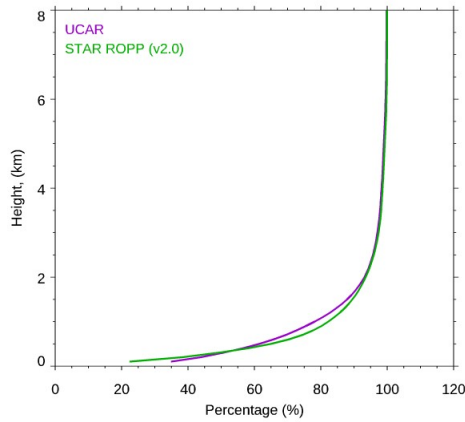


Figure 4. The RO penetration percentage (defined as the observation number at each penetration depth relative to the observation number at 8 km) of STAR ROPP (in green) and UCAR (in purple).

4.2 Stability

The observation number and quality of RO data products may vary with the receiver’s status, changes in processing configuration, the references and criteria used in the quality control procedure, etc. We developed the NOAA STAR Integrated Calibration and Validation System (ICVS) for RO to routinely monitor the quality of multiple RO missions and identify the quality change in the time series of RO data products. (see <https://ncc.nesdis.noaa.gov/GNSSRO/ICVS/index.php>).

Figure 5 showed that the QCed COSMIC-2 number of observations provided by STAR ROPP is similar to or slightly larger than that of UCAR at both 35 km altitude (Figure 5a) and near the surface height (Figure 5b). The jump in May 2021 is because the COSMIC-2 full operational capability (FOC) started.

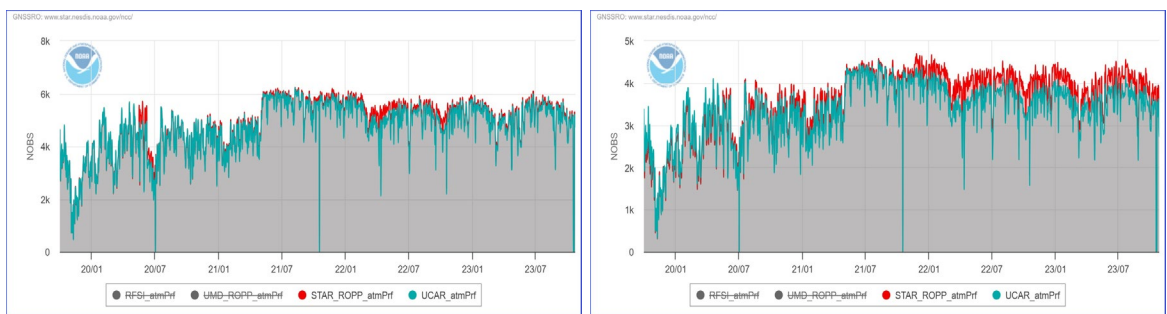


Figure 5. Time series for number of observations passed quality control at (a) 10hPa (~35 km altitude) and (b) 925hPa (~0.8 km altitude). STAR ROPP is in red, and UCAR is in cyan.

Figures 6 and 7 showed the time series of mean bias and standard deviation of the fractional O-B (observation minus background reference) bending angle at 20 km altitude (Figures 6a and 7a) and 3km altitude (Figures 6b and 7b). The sudden jump in the O-B bending angle time

series in Figure 6b and Figure 7b after 24 March 2020 is because COSMIC-2 data was assimilated into ERA-5 on that date. Another noticeable jump in the O-B bending angle standard deviation time series (Figure 7a) is that the UCAR-ERA5 standard deviation decreased after May 14, 2020. We have not fully understood it yet. The first impression is that the geoid file is updated in UCAR’s processing procedure.

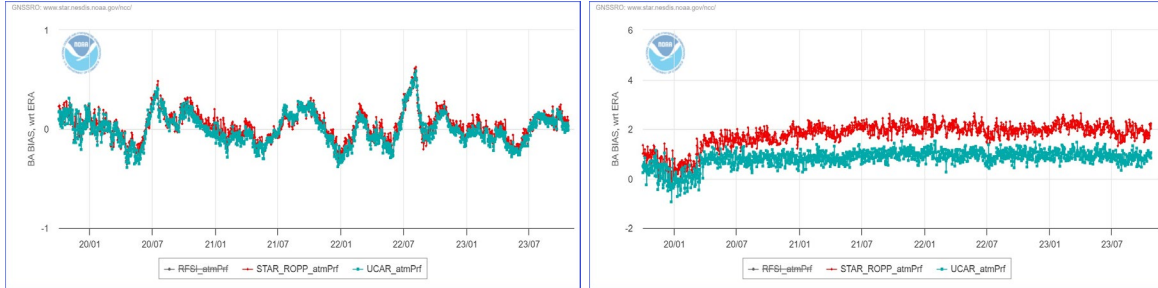


Figure 6. Time series of the fractional difference between COSMIC-2 bending angle and ERA5 simulated bending angle at (a) 50hPa (~20 km altitude) and (b) 700 mb (~3 km altitude). STAR ROPP O-B time series is in red, and UCAR O-B time series in cyan.

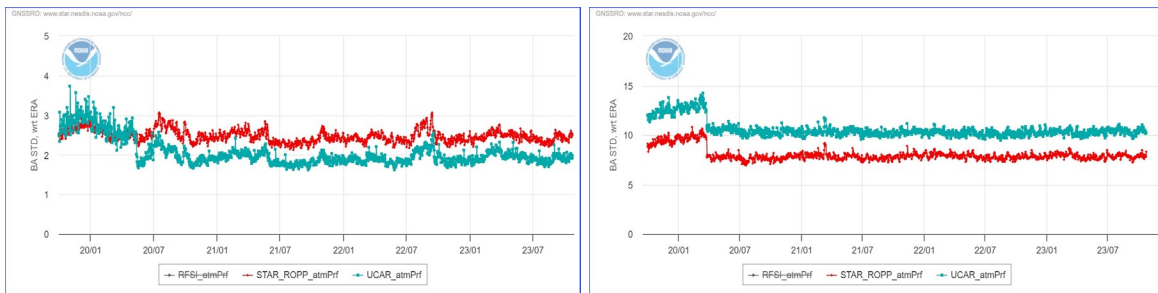


Figure 7. Similar to Figure 6 but for standard deviations.

5. Data format

The main output is stored in NetCDF files (one for each RO measurement). Consistent with the name conversion from other RO processing centers, the output file name has a “atmPrf_” prefix and “_nc” suffix.

The processed output “atmPrf” file contains global variables (Table 2) and derived variables as a function of geometric height (Table 3).

Table 2: The global variables:

Variable	Description
<i>bad</i>	Quality Control Flag; bad = 0 (QC pass), bad > 0 (QC fail)
<i>roc</i>	The local radius of curvature at the reference point (meter)
<i>r_coc</i>	Center of curvature relative to Earth’s center (meter)
<i>time</i>	Time at the reference point (second)
<i>lat</i>	Latitude of the reference point (degree)

<i>lon</i>	Longitude of the reference point (degree)
<i>azim</i>	GNSS->LEO line of sight angle from True North of the reference point (degree)

Table 3: Derived variables as a function of altitude

Variable	Description
<i>impact</i>	Impact parameter (meter)
<i>bangle_L1</i>	Bending angle at L1 band (rad)
<i>bangle_L2</i>	Bending angle at L2 band (rad)
<i>bangle_opt</i>	Ionospheric corrected and optimized bending angle (rad)
$\Delta\alpha/2$	Bending angle uncertainty (half of Local Spectral Width)
<i>alt_refrac</i>	Altitude (meter)
<i>gep_refrac</i>	Geopotential height (meter)
<i>refrac</i>	Refractivity (N unit)
<i>dry_temp</i>	Dry temperature (Kelvin)
<i>lat_tp</i>	Latitude (degree)
<i>lon_tp</i>	Longitude (degree)
<i>azim_tp</i>	GNSS->LEO line of sight angle from True North (degree)

Table 4 lists the key features and notable enhancements introduced in different STAR ROPP retrieval algorithm versions.

Table 4. Summary of key features and enhancements in STAR ROPP versions.

Version	Main Feature and Enhancements	Comments
v.1.0 Mar 2021	1. Input: excess phase from atmPhs/conPhs file 2. QC reference: ERA5 reanalysis	
v.2.0 Nov 2023	1. QC reference: ERA5 six-hour forecast 2. Amplitude threshold scale factor is set to 0.35	<u>Reason:</u> 1. The ERA5 six-hour forecast is used for the QC reference mainly for near-real-time post-processing. 2. The default Amplitude threshold scale factor is 0.5, which rejects too many observations in the near-surface region, leading to shallow penetration depth.

*We only released data generated by Version 2.0.

6. References

1. The Radio Occultation Processing Package (ROPP) Pre-processor Module User Guide, version 10.0, 30 September 2020, the ROM SAF Consortium, Ref: SAF/ROM/METO/UG/ROPP/004
2. Gorbunov, M. E., Lauritsen, K. B., Rhodin, A., Tomassini, M., and Kornblueh, L., Analysis of the CHAMP experimental data on radio-occultation sounding of the earth's atmosphere, *Izvestiya, Atmospheric and Oceanic Physics*, 41, 798–813, 2005.